EXPERIMENTAL AND NUMERICAL MODELLING OF SOIL WATER EVAPORATION.

DAVID A. ENCALADA*

*Universidad Politécnica de Cataluña
Campus Norte UPC, 08034 Barcelona, Spain
e-mail: david.encalada@estudiant.upc.edu

Key words: soil evaporation, evaporation, drying

Abstract. Evaporation is the principal cause of water loss from the soil to the atmosphere. This document provides the experimental results of evaporation on soil samples with small thickness. Two evaporation stages were identified analysing temperature in the soil and evaporation rate. Additionally, the experimental results were compared with CODE_BRIGHT which is a finite element code. The results show that water retention curve is a critical property to define the evaporation stages in the numerical modelling. Also, the boundary conditions are nonlinear and have strong influence on the evaporation stages.

1 INTRODUCTION

Soil water evaporation is the flux of moisture upwards to atmosphere. This process plays an important role in the hydrology cycle and energy balance across land–atmosphere interface. Soil water evaporation is a coupled phenomena that involves the flux of water and heat, and is affected by atmospheric conditions (e.g., temperature, relative humidity, wind and radiation) and soil properties (e.g., hydraulic and thermal properties). The stages in bare soil and in steady conditions are:

1. Stage 1 or constant rate: External conditions control this stage [1, 2]. However, the soil properties control the duration of this stage [2]. Stage 1 happens at the beginning of evaporation when the soil wet and the supply of water to the surface is constant.

2. Stage 2 or falling: This stage starts when the liquid phase becomes discontinuous [3]. Hydraulic soil properties controls this stage [2].

3. Stage 3 or slow rate: When the surface is desiccated the water supply stops. The evaporation occurs below the surface, and the vapour is transported by diffusion

through the dry surface. Diffusion dominates the evaporation rate in this stage [4, 3].

When the climate conditions are not steady, the drying curve can change. Others modifications in the curve are the effect in saline soils [5] and the effect of wind on the surface [6]. Wind on the surface produces a high evaporative demand that causes decreasing evaporation rate in the stage 1.

Soil water evaporation involves two domains. The atmosphere or free flux of air compound by gas phase. The other domain is the multiphase porous media. Usually, transport of water is modelled considering one domain (porous media) with a boundary condition at top. This single domain concept can use single liquid phase [7] or gas and liquid phases [8]. The most advanced model considers two domains concept [9]. However, it was developed to solve the hydro-thermal problem and not includes mechanical coupling.

2 METHODOLOGY

2.1 EXPERIMENT

We carry on a test system to evaluate evaporation on a thin soil sample in room conditions (see Figure 1). Two soil sample with different texture (clay and sand) were tested. They were: (1) Castelldefels Beach sand; (2) Agropolis clay. The Castelldefels Beach sand is fine and uniform sand. This material was selected to represent granular cohesionless soils. Agropolis clay is a low plasticity clay and was chosen to represent fine-grained soils.

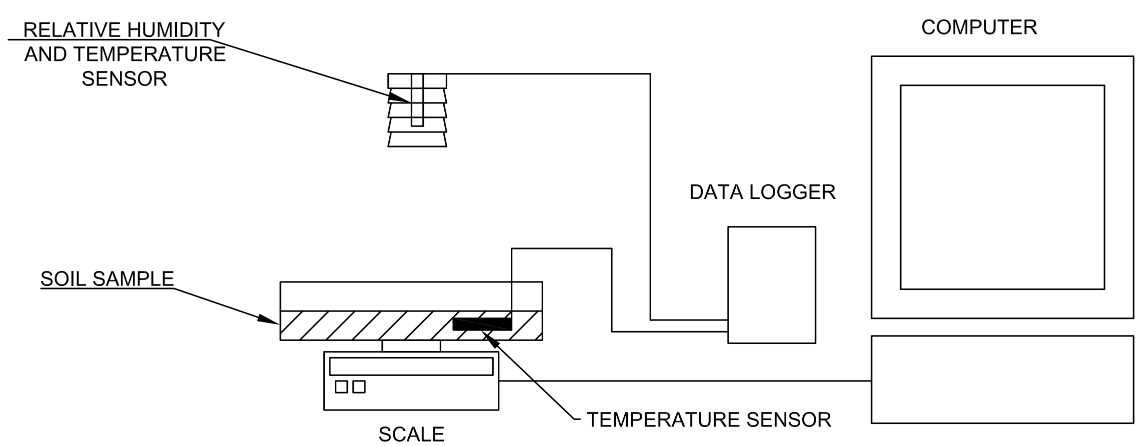

Figure 1: Schematic view of the experimental setup.

The information were collected through a data logger Decagon Em50 and a computer. One temperature sensor Rt-1 (accuracy ±0.5°C from 5°C to 40°C) was inside the sample. A sensor ATMOS 14 measured the temperature and relative humidity of the atmosphere

20 cm above the soil sample. These sensors were connected to Em50 data logger. A tray with dimensions 18.5 and 29.5 cm contained the soil sample of 2 cm thickness. A scale Sartorius 6101-1S was connected to a computer and measured the weight of the sample every 10 min to obtain the water loss and evaporation rate.

2.2 NUMERICAL MODEL

We used CODE_ BIRGHT program to simulate the evaporation on the samples. CODE_ BRIGHT is a finite element code to solve coupled thermo-hydro-mechanical (THM) problems in geological media [8]. This code models a multiphase flow (i.e., solid, liquid and gas) and multicomponent (i.e., water and air). In these models we only considered thermo-hydraulic (TM) formulation. Additionally, we consider that the gradient of gas pressure (P_g) is quite small and thermal diffusivity is generally several hundred times smaller than the air diffusivity [11]. Due to this considerations we ignore the balance equation of the air component. Finally, the equations that we solved are the mass balance of water equation

$$\frac{\partial}{\partial t}(\omega_l^w \rho_l S_l \phi + \omega_g^w \rho_g S_g \phi) + \nabla \cdot (\mathbf{j}_l^w + \mathbf{j}_g^w) = f^w \tag{1}$$

and the internal energy balance equation

$$\frac{\partial}{\partial t}(E_s \rho_s (1-\phi) + E_l \rho_l S_l \phi + E_g \rho_g S_g \phi) + \nabla \cdot (\mathbf{i}_c + \mathbf{j}_{Es} + \mathbf{j}_{El} + \mathbf{j}_{Eg}) = f^Q \tag{2}$$

where f^w is an external supply of water, ϕ is porosity, ω_α^i is the mass fraction of species i in phase α, ρ_α is the density of phase α, S_α is the degree of saturation of phase, E_α is the internal energy in phase α, $\mathbf{i}_c$ is energy flux due to conduction through the porous medium, $\mathbf{j}_{E\alpha}$ are advective fluxes of energy caused by mass motions and f^Q is an internal/external energy supply.

The boundary conditions are considered only on the upper boundary and are the flux of vapour ($\mathbf{j}_g^w$) and the flux of heat ($\mathbf{j}_e$)

$$\mathbf{j}_g^w = (\omega_g^w)^0 j_g^0 + (\omega_g^w)^0 \gamma_g (P_g^0 - P_g) + \beta_g ((\rho_g \omega_g^w)^0 - \rho_g \omega_g^w) \tag{3}$$

$$\mathbf{j}_e = j_e^0 + \gamma_e (T^0 - T) + E_g^w j_g^w + E_g^a j_g^a + E_l^w j_l^w + E_l^a j_l^a \tag{4}$$

where the superscript 0 represent the prescribed values at the soil-atmosphere interface, j_g^0 is the prescribed gas flow, j_e^0 is the prescribed heat flow and γ_g, β_g and γ_e are transfer coefficients. The transfer coefficients β_g and γ_e have a strong influence on the results and characterize the atmosphere behaviour.

3 RESULTS

Figure 2a and 2b shows the experimental results for Agropolis clay and Casteldefels Beach sand, respectively. The relative humidity (RH) oscillated between 0.47 and 0.68 and environmental temperature between 19 and 21.3°C. The temperature on the soil sample is on average 1.3°C below the atmosphere temperature in the first evaporation phase. To analyse the evaporation rate we consider the centered moving average in two hours. We observed two stages of the evaporation. The first stage where the evaporation rate is highly dependent on the RH. Then, the evaporation rate slow down until the specimen completely dries. Also, we see that when the second stage starts, the temperature in the sample starts to increase and goes just above the atmosphere temperature. In this experiment the third stage has not seen. To analyse the third stage, experiments with soil columns and water table recharge should be considered.

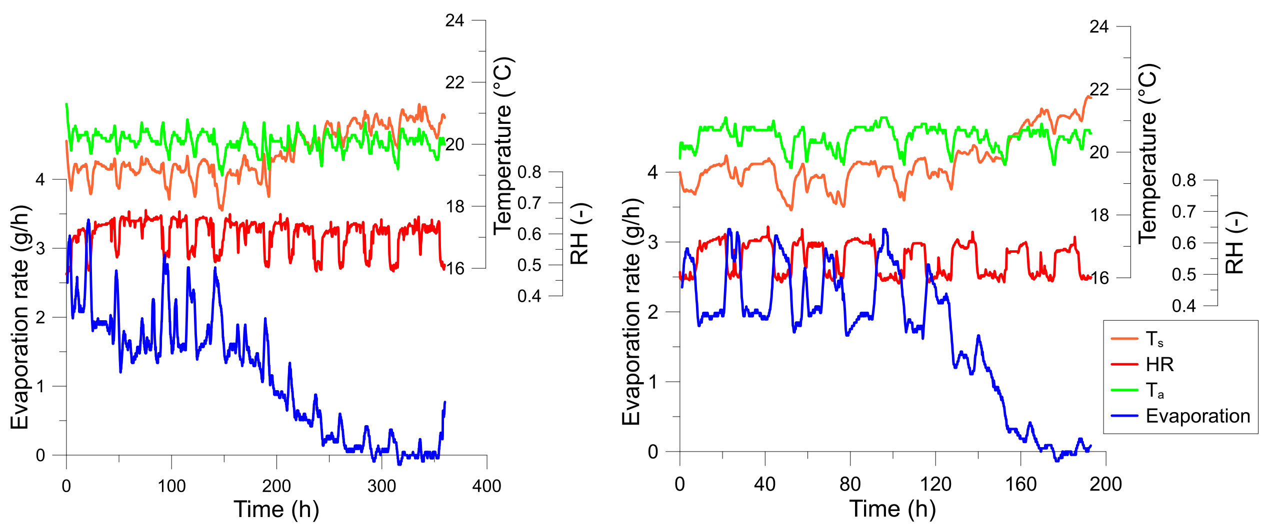

Figure 2: Evaporation rate and environmental conditions during the experiment. (a) Agropolis clay. (b) Casteldefels Beach sand.

The properties, parameters and boundary conditions of the models are summarised in Table 1. The property that has more influence on the drying curves is the water retention parameters. The thermal properties has similar values for sand and clay. The great difference between clay and sand is the difference of hydraulic parameter (i.e., the intrinsec permeability and soil water retention curve). Clay has a higher value of P_0 (0.4 MPa) and k ($1{\cdot}10^{-16}$ m^2). The boundary conditions depends on environmental measurements. The transfer parameters β_g and γ_e were calibrated. The value of γ_e remained constant meanwhile the value of β_g varies with the value of relative humidity. Additionally, to have a better fitting of second evaporation stage the parameter β_g varies with the degree of liquid saturation (S_l) according with the soil surface resistance concept [14].

Figures 3 and 4 compares, respectively, the evaporation rate and water loss of the model with the experiment. The evaporation rate and water loss predictions from the

<table>
<tr><th colspan="2">Parameter</th><th>Clay</th><th>Sand</th></tr>
<tr><td>Porosity</td><td>ϕ (-)</td><td>0.48</td><td>0.38</td></tr>
<tr><td rowspan="5">Retention curve</td><td>λ (-)</td><td>0.4</td><td>0.7</td></tr>
<tr><td>P_0 (MPa)</td><td>0.4</td><td>0.004</td></tr>
<tr><td>σ_0 (N m^{-1})</td><td colspan="2">0.072</td></tr>
<tr><td>S_{rl} (-)</td><td>0.03</td><td>0</td></tr>
<tr><td>S_{ls} (-)</td><td colspan="2">1</td></tr>
<tr><td>Intrinsec permeability</td><td>k (m^2)</td><td>$1{\cdot}10^{-16}$</td><td>$2{\cdot}10^{-12}$</td></tr>
<tr><td rowspan="2">Relative permeability</td><td>λ (-)</td><td colspan="2">6</td></tr>
<tr><td>A (-)</td><td colspan="2">1</td></tr>
<tr><td rowspan="3">Thermal conductivity</td><td>λ_s (W m^{-1} °C^{-1})</td><td colspan="2">2.9</td></tr>
<tr><td>λ_a (W m^{-1} °C^{-1})</td><td colspan="2">0.025</td></tr>
<tr><td>λ_w (W m^{-1} °C^{-1})</td><td colspan="2">0.58</td></tr>
<tr><td>Specific Heat of solid</td><td>C_s (J kg^{-1} °C^{-1})</td><td colspan="2">1000</td></tr>
<tr><td>Solid density</td><td>ρ_s (m s^{-3})</td><td colspan="2">2700</td></tr>
<tr><td>Vapour mass fraction*</td><td>ω_g^w (-)</td><td colspan="2">variable</td></tr>
<tr><td>Gas density*</td><td>ρ_g (m s^{-3})</td><td colspan="2">variable</td></tr>
<tr><td>Temperature</td><td>T^0 (°C)</td><td colspan="2">T_a</td></tr>
<tr><td>Vapour transfer**</td><td>β_g (m s^{-1})</td><td colspan="2">$4.2{\cdot}10^{-3}$-$4.5{\cdot}10^{-3}$RH</td></tr>
<tr><td>Heat transfer</td><td>γ_e (J s^{-1} °C^{-1})</td><td colspan="2">20</td></tr>
</table>

* Depends on T and RH

** Depends on degree of saturation

model are in good agreement with experiment data. The model replicates the influence of the environmental conditions in the first evaporation stage. A nonlinearity on the mass transfer boundary condition has to be include to fit better the second stage

$$\beta_g = \frac{1}{\dfrac{1}{\beta_g^0} + A \cdot e^{-B \cdot S_l}} \tag{5}$$

where β_g^0 is the initial mass transfer coefficient that depends on the environmental conditions and A and B are parameters to fit. Parameter A controls when the second stage starts and is associated with a critical value of degree of liquid saturation (S_{lc}). In the models we used 6000 and 40 for the value of A and B, respectively.

4 CONCLUSIONS

Evaporation is the principal cause of water loss. Geotechnical engineering have paid less attention to this phenomenon. This may be one of the reason for the lack evaporation models in water transport that incorporate mechanical coupling. CODE_BRIGHT solves THM problems. Nevertheless, TH models were used and for future investigations mechanical coupling could be incorporated.

Two evaporation stages are seen in the experimental results. A drop of evaporation rate and a rise of temperature in the soil sample indicate the beginning of second evaporation stage. The first stage is dependent on the atmospheric conditions.

In general the model fits the experimental data. The high sensitivity to atmospheric conditions during first stage is replicated with the model. To replicate the second evaporation stage we include the soil surface resistance definition that creates a nonlinearity on the boundary condition. This makes the mass transfer coefficient a function of degree of saturation.

REFERENCES

[1] Hillel, D. *Introduction to Environmental Soil Physics.* Elsevier Academic Press (2004).

[2] Lehmann, P., Assouline, S. and Or, D. Characteristic lengths affecting evaporative drying of porous media. *Physical Review E - Statistical, Nonlinear, and Soft Matter Physics, 77* (2008) **5**:1–16.

[3] Shokri, N. and Or, D. What determines drying rates at the onset of diffusion controlled stage-2 evaporation from porous media? *Water Resour. Res., 47* (2011) **9**:1–8.

[4] Wilson, G. W., Fredlund, D. G., and Barbour, S. L. The effect of soil suction on evaporative fluxes from soil surfaces. *Can. Geotech. J, 34* (1997) **1**:145–155.

[5] Newson, T. a and Fahey, M. The effect of soil suction on evaporative fluxes from soil surfaces: Discussion. *Can. Geotech. J, 35* (1998) **4**:692–694.

[6] Shahraeeni, E., Lehmann, P., and Or, D. Coupling of evaporative fluxes from drying porous surfaces with air boundary layer: Characteristics of evaporation from discrete pores. *Water Resour. Res., 48* (2012) **9**:1–15.

[7] Simunek, J., Jacques, D., Langergraber, G., Bradford, S. A., Sejna, M. and Van Genuchten, M. T. Numerical modeling of contaminant transport using HYDRUS and its specialized modules. *Journal of the Indian Institute of Science, 93* (2013) **2**:265–284.

[8] Olivella, S., Gens, A., Carrera, J. and Alonso, E. Numerical formulation for a simulator (CODE_BRIGHT) for the coupled analysis of saline media. *Engineering Computations, 13* (1996) **7**:87–112.

[9] Fetzer, T., Smits, K. M. and Helmig, R. Effect of Turbulence and Roughness on Coupled Porous-Medium/Free-Flow Exchange Processes. *Transport in Porous Media, 114* (2016) **2**:1080–1100.

[10] Fredlund, D. G., Rahardjo, H., and Fredlund, M. D. *Unsaturated Soil Mechanics in Engineering Practice*. John Wiley & Sons, Inc (2012).

[11] Lu, Ning and Likos, William J., *Unsaturated Soil Mechanics*. J. Wiley (2004).

[12] Ledesma, A. Cracking in desiccating soils. *E3S Web of Conferences, 9* (2016) 03005.

[13] Wilson, G. W., Fredlund, D. G., and Barbour, S. L. Coupled soil-atmosphere modelling for soil evaporation. *Can. Geotech. J, 31* (1994) **2**:151–161.

[14] van de Griend, A., Owe, M. Coupled soil-atmosphere modelling for soil evaporation. *Water Resources Research, 30* (1994) **2**:181–188.

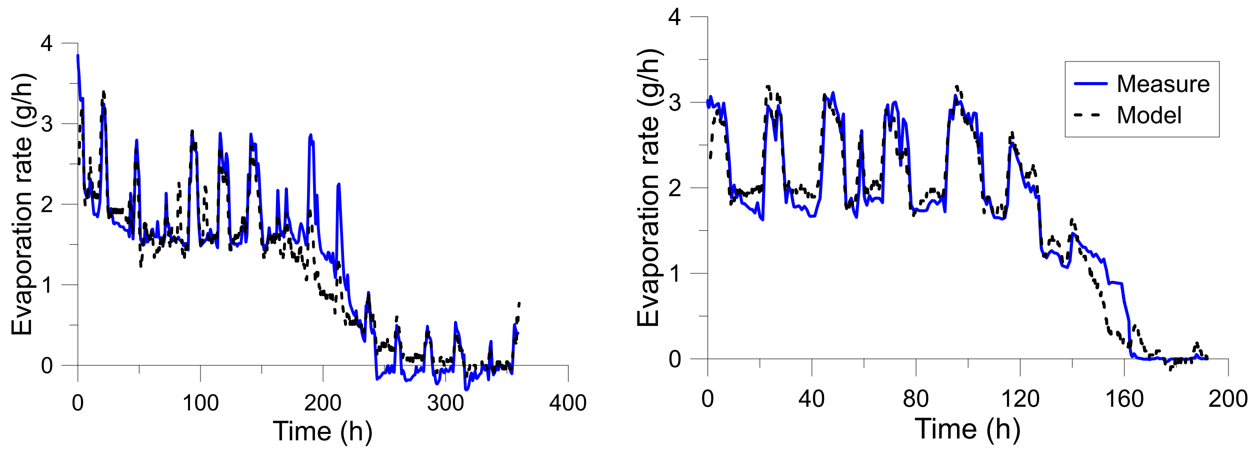

(a) (b)

Figure 3: Evaporation rate. (a) Agropolis clay. (b) Casteldefels Beach sand.

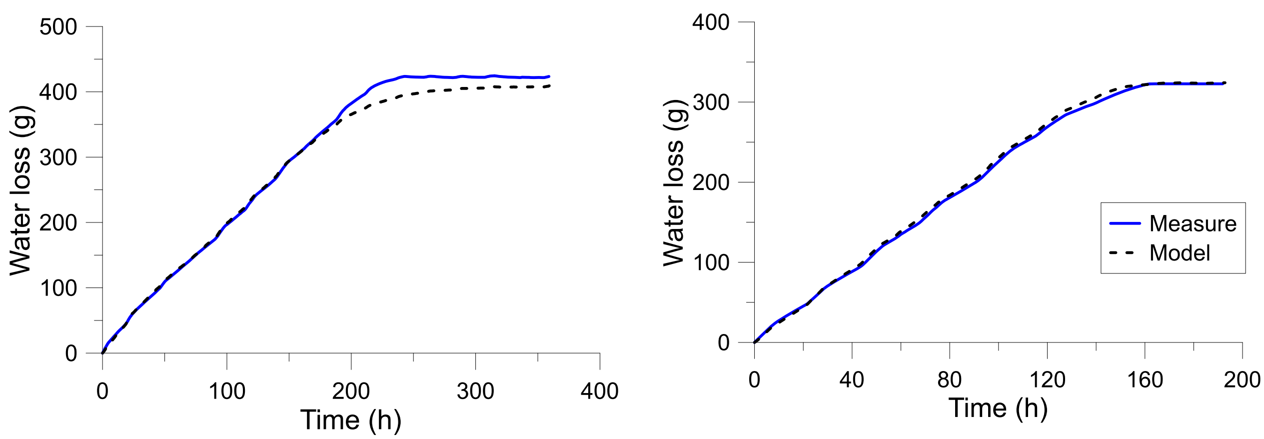

(a) (b)

Figure 4: Water loss. (a) Agropolis clay. (b) Casteldefels Beach sand.